Magnetic Barkhausen Noise for Characterization of Recovery and Recrystallization

Kizkitza Gurruchaga, Ane Martínez-de-Guerenu, Miguel Soto, and Fernando Arizti

CEIT and Tecnun (University of Navarra), 20018 San Sebastián, Spain

The capacity of magnetic Barkhausen noise (MBN) measurements to characterize recovery and the onset and evolution of recrystallization processes occurring during the annealing of cold rolled low carbon steel is analyzed. Cold rolled low carbon steel samples were isothermally annealed at laboratory under different conditions in order to promote various degrees of recovery or recrystallization. The effect of recovery and recrystallization processes on the MBN envelope, the amplitude of the peak of the MBN envelope, the time integral of the MBN envelope and the MBN energy is discussed and related to the microstructural changes produced by these softening processes. The obtained results prove that several parameters derived from the MBN are able to follow the progress of recovery and recrystallization.

Index Terms—**Low carbon steel, magnetic Barkhausen noise, nondestructive testing, recovery, recrystallization.**

I. Introduction

MAGNETIC BARKHAUSEN NOISE (MBN) results from the discontinuous movement of magnetic domain walls (DWs) during magnetization of a polycrystalline ferromagnetic material when the DWs overcome local pinning sites. It is well known that microstructural features, such as dislocation density and the different arrangements of dislocations, distribution and size of grains, grain boundaries, second phase precipitates or even applied or residual stresses act as local pinning sites that strongly hinder the movement of DWs and hence influence the MBN. The MBN is sensitive to the microstructure as these microstructural features affect both the pinning strength and the mean free path of the displacement of DWs during magnetization.

Several earlier studies have successfully analyzed the influence of variations in dislocation density [1]–[3] and average grain size [4], [5] on MBN. Therefore, MBN is expected to be affected by both recovery and recrystallization, due to the changes that these processes produce during annealing treatments on the cold rolled steel microstructure. Recovery involves the rearrangement of dislocations into low energy configurations and the annihilation of dislocations, while recrystallization implies the nucleation and growth of new defect free grains [6].

Earlier studies on a cold rolled low carbon steel showed that some parameters derived from magnetic hysteresis loops can be useful to characterize recovery and to detect the onset of recrystallization [7], [8]. Especially, the coercive field $(\mathrm{H_c})$ is able to follow the progress of recovery processes [7], [9], [10] since it is proportional to the square root of the dislocation density [11]. Moreover, in some cases, when the variation of the effective size of the microstructure during recrystallization is very small, $\mathrm{H_c}$ can also be employed to characterize the progress of recrystallization [7]. Following these studies, this paper researches into the use of some other parameters derived from MBN measurements for the nondestructive characterization of recovery and recrystallization during the annealing of this cold rolled steel.

Manuscript received June 18, 2009; revised July 22, 2009; accepted July 23, 2009. Current version published January 20, 2010. Corresponding author: A. Martínez-de-Guerenu (e-mail: amartinez@ceit.es).

Digital Object Identifier 10.1109/TMAG.2009.2029069

II. Experimental Procedure

An industrially produced extra low carbon steel, cold rolled to a final thickness of 0.53 mm through a reduction of 76% and a hot band grain size of 12 μm was used in this study. The chemical composition of the steel in wt % was: 0.03C—0.38Mn—0.0004S—0.11Si—0.037P—0.035Al—0.004N. Samples (200 mm long $\times$ 14 mm wide) cut perpendicular to the rolling direction of the cold rolled sheet, were isothermally annealed at laboratory at low temperatures, 300, 400, and 500°C, in order to promote recovery and avoid interaction with recrystallization, and at a higher temperature, 575°C, in order to produce samples with various degrees of recrystallization [7].

The MBN measurements were made using a system designed and constructed at the authors' laboratory [12]. The Barkhausen emission was detected with a small 50 turn encircling search coil surrounding the sample. The tangential magnetic field strength $(\mathrm{H_t})$ was measured by a Honeywell solid-state SS495A1 Hall sensor placed at the surface of the samples next to the pickup coil. Near saturation MBN was measured applying sinusoidal magnetic field strengths of about 4.1 kA/m at 0.1 Hz. The MBN was filtered with a band-pass filter with cut off frequencies of 1 kHz and 25 kHz.

The samples were demagnetized at the test frequency prior to each test by applying a sinusoidal signal whose amplitude diminished gradually, in several cycles, to values close to zero. The MBN activity was characterized by the MBN envelope or root-mean-square RMS profile of MBN $(\mathrm{MBN_{env}})$, represented as a function of the measured $\mathrm{H_t}$; the amplitude of the peak of the $\mathrm{MBN_{env}}(\mathrm{MBN_{env\_max}})$; the time integral of the $\mathrm{MBN_{env}}(\mathrm{Int}(\mathrm{MBN_{env}}))$, which represents the area below the envelope over a semi-period of magnetizing cycle; and by the Barkhausen noise energy $(\mathrm{MBN_{energy}})$, which is computed by integrating the time dependence of the squared raw MBN signal over a semi-period of magnetizing cycle [3].

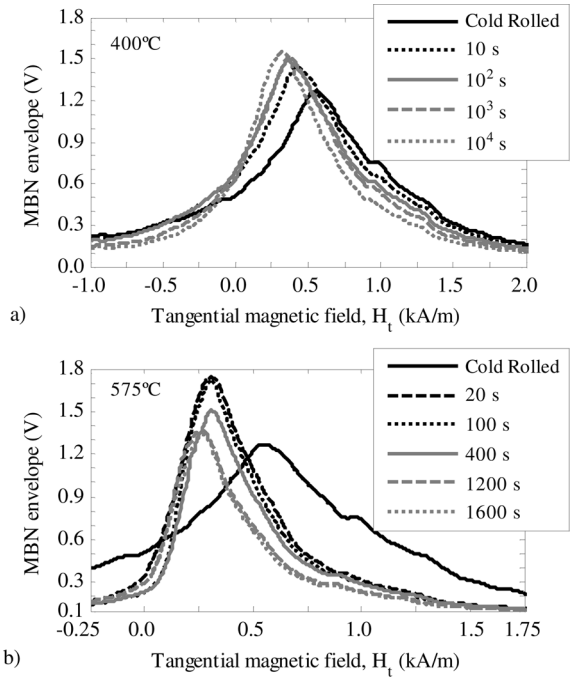

Fig. 1. MBN envelope (RMS profile) as a function of the tangential magnetic field, $(\mathrm{H_t})$ during the annealing at: (a) 400°C and (b) 575°C.

III. Results and Discussion

Fig. 1(a) and (b) shows the MBN envelopes $(\mathrm{MBN_{env}})$ as a function of $\mathrm{H_t}$ for various annealing states at 400°C and 575°C, respectively. The $\mathrm{MBN_{env}}$ of the cold rolled sample is shown as reference in both figures. It can be seen that the MBN envelopes show a single peak, which can be attributed to the single ferritic phase of this steel. At temperatures in the range 300–500°C, as the annealing time increases a narrower peak is observed, the amplitude of the peak increasing steadily and its position shifting to lower magnetic field values. However, after 20 s at 575°C a continuous decrease of the amplitude of the peak with increasing annealing time is obtained.

The evolution of the amplitude of the peak of the $\mathrm{MBN_{env}}(\mathrm{MBN_{env\_max}})$ as a function of annealing time is shown in Fig. 2, in logarithmic scale for the analyzed annealing temperatures. At low annealing temperatures (300–500°C) a progressive increasing tendency of $\mathrm{MBN_{env\_max}}$ with annealing time is observed. At these temperatures (up to 3160 s at 500°C), only recovery processes take place in the steel substructure [7]. This increasing trend is consistent with the results reported in [1] where a reduction of the $\mathrm{MBN_{env\_max}}$ is observed due to the increase in dislocation density caused by tensile deformation. On the one hand, the reduction in the dislocation density caused by recovery processes reduces the number of pinning sites for DWs. This effect would reduce the number of Barkhausen jumps, which could reduce the $\mathrm{MBN_{env\_max}}$. On the other hand, when the dislocation density decreases the distances of the movements of the DWs become larger, causing pulses of larger amplitudes [3]. The increasing tendency of $\mathrm{MBN_{env\_max}}$ found here would indicate that the increase of the distance of DW movements would have a predominant effect on $\mathrm{MBN_{env\_max}}$.

After 100 s at 575°C, $\mathrm{MBN_{env\_max}}$ starts to decrease, and diminishes gradually with the progress of recrystallization at this

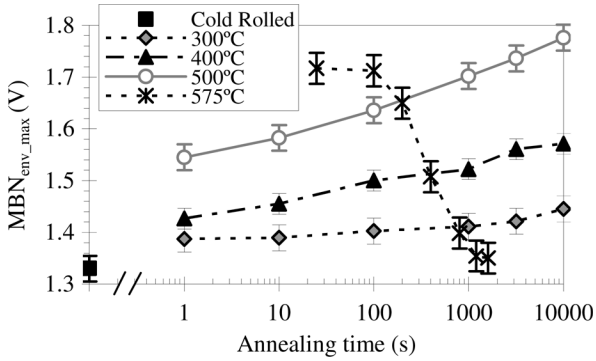

Fig. 2. Amplitude of the peak of the MBN envelope $(\mathrm{MBN_{env\_max}})$ as a function of annealing time.

temperature (the evolution of the recrystallized fraction $(\mathrm{X_v})$ at 575°C is shown in Fig. 3, [7]). It has to be taken into account that during recrystallization more than one microstructural element varies and hence all may affect to the DW movements. According to the behaviour during recovery, the decrease in the average dislocation density produced by the movement of the recrystallization front through the material should lead to increasing $\mathrm{MBN_{env\_max}}$ values. However, $\mathrm{MBN_{env\_max}}$ is observed to continuosly decrease during recrystallization. When recrystallization starts (see inset (a) in Fig. 3), only a few new recrystallized grains of small size start to appear, the microstructure being mainly formed by the deformed grains, free after recovery from the high dislocation density caused by cold rolling. Although during recrystallization there is not a significant change in the recrystallized mean grain size in this steel [7], the deformed areas still containing the nonrecrystallized but recovered elongated grains diminish their size as they are substituted by the new recrystallized grains (see micrograph in inset (b) in Fig. 3). After the recovery processes have taken place, the deformed grains contain much lower dislocation density and the grain boundaries of these elongated grains start to be the predominant microstructural feature hindering the largest DW movements. Therefore, if the $\mathrm{MBN_{env\_max}}$ parameter is considered as representative of the largest amplitude of the MBN and of the largest jumps of the DWs, the decrease of the $\mathrm{MBN_{env\_max}}$ during recrystallization can be explained by the gradual reduction of the size of the recovered areas as they are substituted by the recrystallized grains. This would mean that also in the case of recrystallization the reduction of the distance of the DW movements has a predominant effect on $\mathrm{MBN_{env\_max}}$. Additionally, the opposite evolution of this parameter during recovery and recrystallization could be used to distinguish between both processes.

Fig. 4 shows the relationship between $\mathrm{MBN_{env\_max}}$ and the $\mathrm{H_c}$ measurements [7] for the whole annealing time range. A linear relationship is obtained between both parameters at the lowest annealing temperatures, up to 3160 s at 500°C and up to 200 s at 575°C (when recrystallization starts). This correlation demonstrates the capacity of this parameter to follow the recovery processes. As soon as the recrystallization is activated, the same relationship is no longer satisfied. The loss of this linear relationship can be explained considering the different microstructural features that are changing during recrystallization and affect each of the parameters. $\mathrm{H_c}$ is a macroscopic measurement and it is affected by the mean grain size [13] (effec-

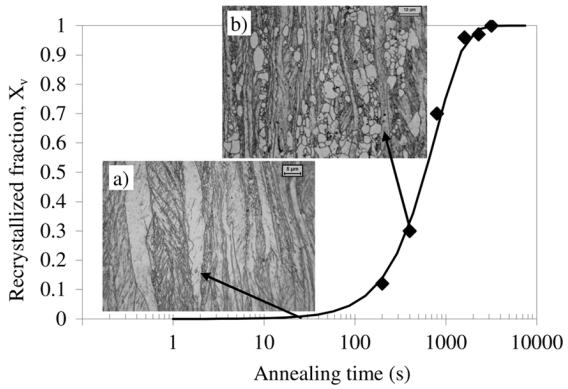

Fig. 3. Evolution of recrystallized fraction $(\mathrm{X_v})$ with annealing time at 575°C, showing the evolution of microstructure at various stages.

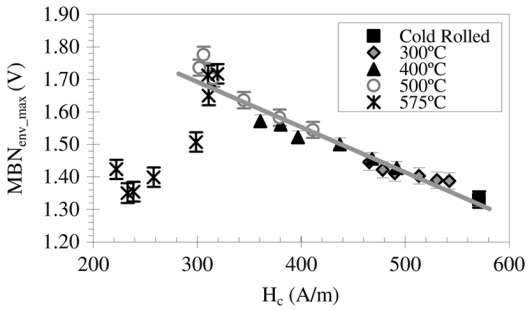

Fig. 4. Correlation between the amplitude of the peak of the MBN envelope, $(\mathrm{MBN_{env\_max}})$ with the coercive field $(\mathrm{H_c})$ for the analyzed temperatures.

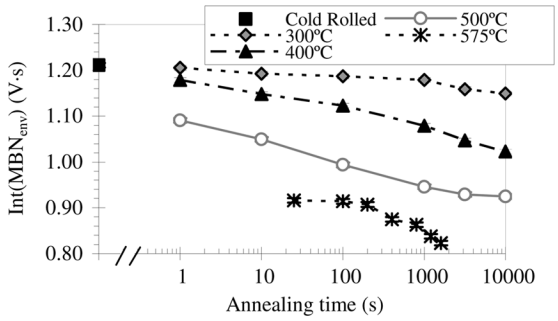

Fig. 5. Time integral of the MBN envelope $(\mathrm{Int(MBN_{env})})$ as a function of annealing time.

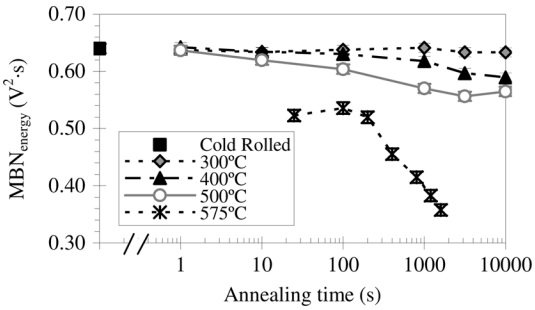

Fig. 6. Energy of the MBN $(\mathrm{MBN_{energy}})$ as a function of annealing time.

tive mean linear intercept length for partially recrystallized microstructures [7]) and by the average dislocation density [11], whereas $\mathrm{MBN_{env\_max}}$ is a microscopic parameter representative of the largest jumps of the DWs and hence of the maximum free path between the microstructural obstacles hindering the DW movements, in this case, the distance between the grain boundaries of the recovered nonrecrystallized areas.

Fig. 5 shows the $\mathrm{Int(MBN_{env})}$ as a function of annealing time. At the lowest temperatures, 300–400°C, $\mathrm{Int(MBN_{env})}$ decreases progressively with annealing time; At 500°C, $\mathrm{Int(MBN_{env})}$ initially follows this same trend, but stagnates for annealing times higher than 3160 s; At 575°C, $\mathrm{Int(MBN_{env})}$ stagnates for annealing times between 25 and 200 s, and decreases more rapidly afterwards with the progress of recrystallization. Comparing the evolution of the $\mathrm{Int(MBN_{env})}$ to that of the $\mathrm{MBN_{env\_max}}$, it can be said that at the lowest annealing temperatures (300–400°C and up to 3160 s at 500°C) the evolution of the $\mathrm{Int(MBN_{env})}$ is similar, in the opposite direction, and provides a smaller standard deviation in the measurement. The reduction of the $\mathrm{Int(MBN_{env})}$ can be explained because although the $\mathrm{MBN_{env\_max}}$ increases, the $\mathrm{MBN_{env}}$ is gradually narrowed as the annealing time increases and the average dislocation density diminishes. Additionally, a linear correlation between $\mathrm{Int(MBN_{env})}$ and $\mathrm{H_c}$ is also obtained and hence, it could also be used to monitor recovery.

However, the stagnation of the $\mathrm{Int(MBN_{env})}$, both between 3160 s and 10000 s at 500°C and in the range 25–100 s at 575°C shows the higher sensitivity of this parameter to the onset of recrystallization (see Fig. 3). After 10000 s at 500°C, the high angle boundary map from EBSD images (see Fig. 6(b) in [7]) showed the presence of several small crystallites a few microns in size surrounded by well defined high angle boundaries, revealing the onset of recrystallization at this temperature. The higher sensitivity of $\mathrm{Int(MBN_{env})}$ can be explained by the influence on this parameter of the small pulses located at the sides of $\mathrm{MBN_{env}}$, near to the saturation regions of the material.

The $\mathrm{MBN_{energy}}$ as a function of annealing time is shown in Fig. 6. At low annealing temperatures or times (300°C and up to 1000 s at 400°C) the value of $\mathrm{MBN_{energy}}$ remains almost constant. At 500°C, initially decreases with annealing time, but slightly increases for annealing times higher than 3160 s. At 575°C, between 25 and 100 s, $\mathrm{MBN_{energy}}$ slightly increases but decreases abruptly afterwards with time. Hence, it is observed that $\mathrm{MBN_{energy}}$ is less sensitive to the initial stages of recovery than $\mathrm{Int(MBN_{env})}$ and $\mathrm{MBN_{env\_max}}$. On the contrary, $\mathrm{MBN_{energy}}$ is more sensitive to the onset of recrystallization, as it responses with an increase of the parameter both after 3160 s of annealing at 500°C and between 25 s and 100 s at 575°C. This effect can be explained taking into account that in the $\mathrm{Int(MBN_{env})}$ both the region of the peak of the $\mathrm{MBN_{env}}$ and the side regions (corresponding to the near saturation regions) have equal influence. In the $\mathrm{MBN_{energy}}$ the central region with pulses of higher amplitudes have more influence as the MBN pulses are squared to calculate the energy. This enhances the capability of this parameter to follow the progress of recrystallization, but reduces the sensitivity for recovery, as during recovery the increase in the energy due to the increase of the pulses of highest amplitude is compensated by the decrease in energy that the narrowing of the $\mathrm{MBN_{env}}$ causes.

The correlations between $\mathrm{MBN_{env\_max}}$ and $\mathrm{MBN_{energy}}$ with the recrystallized fraction $(\mathrm{X_v})$ are shown in the left and right vertical axes of Fig. 7, respectively. It can be seen that linear correlations between these parameters and $\mathrm{X_v}$ are satisfied, so

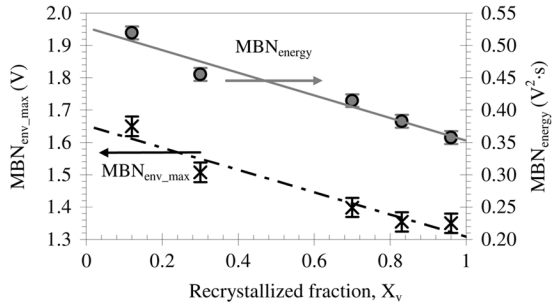

Fig. 7. Correlation between the amplitude of the peak of the MBN envelope, $(\mathrm{MBN_{env\_max}})$ and the energy of the MBN signal $(\mathrm{MBN_{energy}})$ with the recrystallized fraction $(\mathrm{X_v})$ at 575°C.

at first it could be said that both parameters could be able to characterize the recrystallization. Although $\mathrm{MBN_{env\_max}}$ has been used to characterize different microstructural features [3], [5], in this case, the error of the measurement of $\mathrm{MBN_{env\_max}}$ in each annealed state relative to the maximum change of this measurement in the overall study is of 8%, while the error of $\mathrm{MBN_{energy}}$ is of 3%. Therefore, the $\mathrm{MBN_{energy}}$ offers a more precise measurement and a better correlation to characterize the recrystallization.

IV. Conclusion

The main microstructural feature hindering the DW movements during the recovery of heavily cold rolled low carbon steel are the dislocations. The amplitude of the peak of MBN envelope $(\mathrm{MBN_{env\_max}})$ and the integral below the MBN envelope $(\mathrm{Int(MBN_{env})})$ can be useful to monitor recovery, due to its sensitivity to the reduction in the average dislocation density.

The $\mathrm{Int(MBN_{env})}$ and the $\mathrm{MBN_{energy}}$ can detect the onset of recrystallization. The main microstructural feature hindering the DW movements during recrystallization and affecting $\mathrm{MBN_{env\_max}}$ are the grain boundaries of the recovered nonrecrystallized areas. The opposite evolution with annealing time of $\mathrm{MBN_{env\_max}}$ during recovery and recrystallization could be used to distinguish between both processes. The $\mathrm{MBN_{env\_max}}$ and the $\mathrm{MBN_{energy}}$ are also able to follow the progress of recrystallization, the $\mathrm{MBN_{energy}}$ presenting higher measurement accuracy.

Acknowledgment

This work was supported by the Ministry of Science and Innovation of Spain (MAT 2006-05805). K. Gurruchaga's and M. Soto's contracts were funded by the Ministry of Science and Innovation of Spain within the framework of the Torres Quevedo Programme and co-funded by the European Social Fund.

References

[1] V. E. Iordache, E. Hug, and N. Buiron, "Magnetic behaviour versus tensile deformation mechanisms in a non-oriented Fe-(3 wt.%)Si steel," *Mater. Sci. Eng. A*, vol. 359, pp. 62–74, 2003.

[2] J. Pal'a, O. Stupakov, J. Bydzovský, I. Tomás, and V. Novák, "Magnetic behaviour of low-carbon steel in parallel and perpendicular directions to tensile deformation," *J. Magn. Magn. Mater.*, vol. 310, pp. 57–62, 2007.

[3] H. Kikuchi, K. Ara, Y. Kamada, and S. Kobayashi, "Effect of microstructure changes on Barkhausen noise properties and hysteresis loop in cold rolled low carbon steel," *IEEE Trans. Magn.*, vol. 45, no. 6, pp. 2744–2747, Jun. 2009.

[4] M. Komatsubara and J. L. Porteseil, "Influence of grain size and strain on Barkhausen noise power of non-oriented silicon steel," *IEEE Trans. Magn.*, vol. 23, no. 5, pp. 3506–3508, Sep. 1987.

[5] R. Ranjan, D. C. Jiles, and P. K. Rastogi, "Magnetic properties of decarburized steels: An investigation of the effects of grain size and carbon content," *IEEE Trans. Magn.*, vol. 23, no. 2, pp. 1869–1876, Mar. 1987.

[6] F. J. Humphreys and M. Hatherly, *Recrystallization and Related Annealing Phenomena*, 1st ed. Oxford, U.K.: Pergamon, 1996.

[7] M. Oyarzabal, K. Gurruchaga, A. Martínez-De-Guerenu, and I. Gutiérrez, "Sensitivity of conventional and non-destructive characterization techniques to recovery and recrystallization," *ISIJ Int.*, vol. 47, no. 10, pp. 1458–1464, 2007.

[8] K. Gurruchaga, A. Martínez-De-Guerenu, M. Soto, and F. Arizti, "Efficacy of magnetic inductive parameters for annealing characterization of cold rolled low carbon steel," *IEEE Trans. Magn.*, vol. 44, no. 11, pp. 3839–3842, Nov. 2008.

[9] A. Martínez-de-Guerenu, F. Arizti, M. Díaz-Fuentes, and I. Gutiérrez, "Recovery during annealing in a cold rolled low carbon steel. Part I: Kinetics and microstructural characterization," *Acta. Mater.*, vol. 52, no. 12, pp. 3657–3664, 2004.

[10] A. Martínez-de-Guerenu, F. Arizti, and I. Gutiérrez, "Recovery during annealing in a cold rolled low carbon steel. Part II: Modelling the kinetics," *Acta. Mater.*, vol. 52, no. 12, pp. 3665–3670, 2004.

[11] H. Traüble, , A. E. Berkowitz and E. Kneller, Eds., "The influence of crystal defects on magnetization processes in ferromagnetic single crystals," in *Magnetism and Metallurgy*. New York: Academic, 1969, vol. 2, p. 621.

[12] A. Martínez-de-Guerenu, K. Gurruchaga, and F. Arizti, "Use of magnetic techniques for characterisation of the microstructure evolution during the annealing of low carbon steels," in *9th Eur. Conf. Non-Destructive Testing (ECNDT)*, Berlin, Germany, 2006.

[13] A. Mager, "Über den einfluss der korngrosse auf die koerzitivkraft," *Ann Phys 6 F Lpz*, vol. 11, no. 1, pp. 15–16, 1952.